Inhibitory cross-talk between P2X and NMDA receptors

Larry Rodriguez[1], Catherine Yi[1], Cameron Chu[1], Quentin Duriez[2,3], Sharyse Watanabe[1], Megan Ryu[1], Brandon Reyes[1], Liana Asatryan[4], Eric Boué-Grabot [2,3] and Daryl Davies[4]*

[1]Department of Pharmacology and Pharmaceutical Sciences, School of Pharmacy, University of Southern California Los Angeles, CA 90033; (L.R.) larryrod@usc.edu; (C.Y) yich@usc.edu; (C.C.) chucamer@usc.edu; (S.W.) sharysew@usc.edu; (M.R.) meganryu@usc.edu; (B.R.) branreyes2970@gmail.com;

[2]Univ. de Bordeaux, Institut des Maladies Neurodégénératives, UMR 5293, F-33000 Bordeaux, France

[3] CNRS, Institut des Maladies Neurodégénératives, UMR 5293, F-33000 Bordeaux, France ; (Q.D) quentinduriez@protonmail.com; (E.B-G) eric.boue-grabot@u-bordeaux.fr,

[4] Titus Family Department of Clinical Pharmacy, School of Pharmacy, University of Southern California Los Angeles, CA 90033; (L.A.) asatryan@usc.edu

* Correspondence: ddavies@usc.edu; Tel.: +1-(323)-442-1427 (D.D.)

Abstract: Purinergic P2X receptors (P2X) are ATP-gated ion channels widely expressed in the CNS. While the direct contribution of P2X to synaptic transmission is uncertain, P2X reportedly affect N-methyl-D-aspartate receptor (NMDAR) activity, which has given rise to competing theories on the role of P2X in the modulation of synapses. However, P2X have also been shown to participate in receptor cross-talk: an interaction where one receptor (e.g. P2X2) directly influences the activity of another (e.g. nicotinic, 5-HT3 or GABA receptors.) In this study, we tested for interactions between P2X2 or P2X4 and NMDARs. Using two-electrode voltage-clamp electrophysiology experiments in *Xenopus laevis* oocytes, we demonstrate that both P2X2 and P2X4 interact with NMDARs in an inhibitory manner. When investigating the molecular domains responsible for this phenomenon, we found that the P2X2 c-terminus (CT) could interfere with both P2X2 and P2X4 interactions with NMDARs. We also report that 11 distal CT residues on the P2X4 facilitate the P2X4-NMDAR interaction, and that a peptide consisting of these P2X4 CT residues (11C) can disrupt the interaction between NMDARs and P2X2 or P2X4. Collectively, these results provide new evidence for the modulatory nature of P2X2 and P2X4, suggesting they might play a more nuanced role in the CNS.

Keywords: NMDA receptors; P2X2 receptors; P2X4 receptors; cross-talk;

1. Introduction

Ionotropic receptors are ligand-gated ion channels (LGICs) responsible for various physiological processes. These LGICs, widely expressed in neurons, are activated by specific chemical species, such as glutamate, adenosine triphosphate (ATP), or γ-aminobutyric acid (GABA), with multiple receptor families being found across diverse population of cells types [1]. Glutamate receptors are one of the largest and most widely expressed family of excitatory LGICs found in the CNS. Three different classes of ionotropic glutamate receptors exist, differentiated by their ability to be stimulated by selective agonists: Kainate, α-amino-3-hydroxy-5-methyl-4-isoxazolepropionic acid (or AMPA), and N-methyl-D-aspartate (or NMDA) receptors. NMDA receptors are heterotetramers, usually consisting of two obligate GluN1 subunits, and either two GluN2 or two GluN3 subunits. Within the NMDA type of glutamate receptors, there exist several subtypes of GluN2 (i.e., GluN2A-D), each with a different cytoplasmic domain, resulting in differences in functional and physiological activities [1, 2].

ATP is an important signaling molecule in the CNS, as it activates P2 receptors, including the ATP-gated cation channel family (P2X receptors) which have been shown to play a role in neuroinflammation, pain, and neurological dysfunction. Among the members of the P2X family (consisting of P2X1-P2X7), P2X2, P2X4, and P2X6 subtypes are generally expressed on most neurons, and are regularly found at the edge of the post-synaptic densities of excitatory synapses [3]. P2X subtypes also show similar structural characteristics: an amino-terminal intracellular domain, two

transmembrane domains, and a carboxy-terminal (CT) intracellular domain. In fact, the closed and open zebrafish P2X4 crystal structures (PDB: 4DW0 and 4DW1, respectively) have previously been used to build other P2X structural models, namely P2X2, highlighting the conserved shape of P2Xs [3].

While ATP is released by neurons (as well as by glial cells in the CNS), direct evidence supporting the function of P2X in synaptic transmission is limited. ATP can be coreleased with GABA or glutamate at central synapse [4] [5], suggesting a modulatory role in synaptic activity or plasticity in the brain. For example, studies on P2X4 knockout (P2X4 KO) mice suggested that calcium entry via P2X4 played a role in the induction of long-term potentiation (LTP) via modulation NMDARs [6]. Additional studies on P2X4 KO mice support the notion that P2X4 modulates NMDARs, although results indicated that calcium influx from P2X4 alone was not sufficient to explain changes in synaptic plasticity [7]. More recent studies reported that P2X can down-regulate NMDARs in a calcium-dependent manner [8], raising more questions regarding the mechanistic function of P2X4. Roles for P2X4 in behavior have continued to emerge; studies have found that P2X4 KO mice 1) show cognitive-behavioral deficits, 2) consume significantly more ethanol as compared to wildtype controls and 3) display aberrant signaling within the mesolimbic pathway of the brain [9-11]. Moreover, pharmacologic and genetic studies support the significance of P2X4 in cognitive function (for a detailed review on P2X modulators in disease, see [12]; P2X4 positive allosteric modulators (e.g., ivermectin and moxidectin) have been shown to reduce ethanol intake in wildtype, [13, 14] and internalization-deficient P2X4 knock-in mice, which display increased surface expression of P2X4, demonstrate that P2X4 regulates anxiety and memory processes [15]. Indeed, increased P2X4 surface expression in excitatory neurons was shown to alter long-term depression and long-term potentiation (LTD and LTP) in the hippocampus, consistent with the idea that post-synaptic P2X4 receptors may regulate NMDAR function. While these studies indicate that P2X are integral in neuronal signaling and cognitive disease states, determining how P2X mediate these effects is necessary for determining their promise as a target for cognitive pathologies (for a recent review of P2X4 in the nervous system, see [16].).

A large body of evidence suggests that a major function of P2X involves interacting with and regulating other LGICs (i.e. cross-talk.) In cross-talk, coactivation of P2X and another receptor leads to rapid inhibition of agonist-evoked currents. P2X cross-talk can rely on physical interactions between the intracellular domains of each receptors and may also regulate the subcellular targeting of receptors in neurons. Cross-talk between several P2X subtypes has been shown to modulate the activity of GABA receptors [17-20], nicotinic ACh receptors [21] and 5-HT3 receptors [22-24]. Alternatively, P2X can also have slow but long-lasting modulatory effects on the function or surface trafficking of receptors; activation of post-synaptic P2X by ATP released from glia has been shown to trigger changes in the surface trafficking of AMPAR, which leads to long lasting changes in synaptic efficacy at glutamatergic synapses. In the hypothalamus, activation of P2X7 by ATP led to increases in the number of surface AMPAR and synaptic strength [25]. In the hippocampus, activation of post-synaptic P2X2 or P2X4 can activate surface AMPAR internalization, leading to a P2X-mediated long term synaptic depression [26, 27]. Despite evidence of the modulatory potential of P2X, interactions between P2X and NMDAR have not been investigated.

To better understand how P2X regulate NMDAR function [6, 7, 28] here we investigated putative interactions between P2X and NMDAR using two-electrode voltage clamp (TEVC) electrophysiology in *Xenopus laevis* oocytes coexpressing P2X2 or P2X4 and various GluN2-containing NMDAR combinations. We demonstrate an interaction between P2X and NMDARs, producing inhibitory responses, and that this interaction between both receptor types exhibits subunit-dependent properties. Using mutagenesis and molecular biology approaches, we delved deeper into the domains responsible for this interaction and found evidence that suggests that the C-terminal of P2X is important for the interactions between P2X and NMDARs.

2. Results

2.1. Coactivation of P2X and NMDA receptors

ATP and glutamate (Glu) are coreleased from presynaptic vessicles [4], suggesting that activation of post-synaptic P2X and NMDARs might occur at the same time. We expressed P2X and NMDARs separately or in combination in *Xenopus laevis* oocytes. Voltage clamp recordings demonstrate that coexpression did not affect either ATP or Glu concentration-responses when tested separately (Figure A1.) Furthermore, ATP did not affect NMDAR responses when expressed alone, and Glu did not affect P2X responses when expressed alone (Figure A2). Note that since NMDARs are heterotetramers consisting of obligate GluN1 and variable GluN2 subunits, we will refer only to the variable GluN2 subunit when discussing differences among NMDARs.

We sought to characterize the effects of activating both receptor types at the same time (coactivation). If both receptors are functionally independent, then simultaneous activation of P2X and NMDAR should be additive. That is, equal to the sum of the separate response of each receptor when activated individually by their respective agonist [17, 20-22]. On the other hand, non-additive responses during concomitant application of both agonists would indicate a functional interaction with synergistic (greater than additive responses) or inhibitory (less than additive response) effects.

2.1.1. Coactivation of P2X4 and NMDA receptors produces non-additive (inhibitory) responses

As presented in Figure 1A, coapplication of both agonists on oocytes coexpressing P2X4 and NMDARs consisting of GluN2B subunits produced a significantly lower current response (black line) than the arithmetic sum of the separate responses evoked by application of Glu and ATP alone (grey line.) The bar graph presented in Figure 1B illustrates the mean of the predicted sum of the Glu responses (white) and ATP responses (black) and mean of actual peak currents evoked during coactivation of P2X4 and different GluN2-containing NMDARs (grey), normalized to the predicted response (set as 100%). Regardless of the GluN2 subunit, we found that coactivation of P2X4 and NMDARs produced significantly smaller responses than predicted: GluN2A, GluN2B, and GluN2C produced 73.6 ± 3.1 % ($p < 0.0001$; n = 9), 77.7 ± 3.9 % ($p < 0.001$; n = 9), and 82.2 ± 4.7 % ($p < 0.01$; n = 10) of the predicted coactivation response, respectively. These results indicate that P2X4 and NMDARs do not function in isolation and that coactivation led to inhibitory responses, independent of the GluN2 subunit composition of NMDARs (One-way ANOVA, $p > 0.05$). Interestingly, we observed an increase in Glu responses after coactivation for GluN2A- and GluN2C-containing NMDARs (GluN2B was not assessed). Unfortunately, due to this non-recovery (i.e. return to baseline) of NMDARs, determining the directional nature of this interaction (i.e. coactivation of P2X4 and then NMDARs, or vice versa) was not further investigated in this current work (see Figure 2C-D).

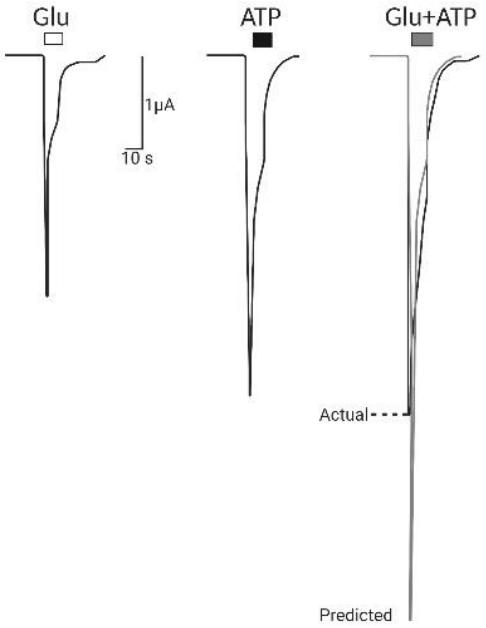

(**a**)

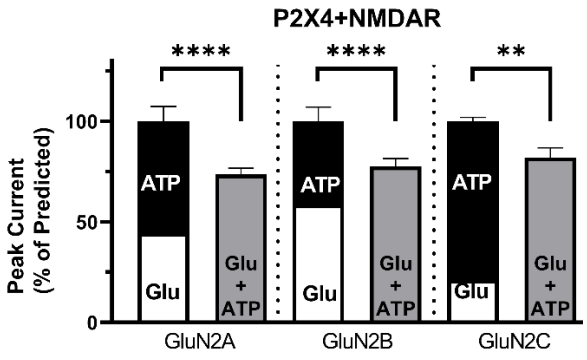

(**b**)

Figure 1. P2X4-NMDAR coactivation produces an inhibited response. **(a)** Representative currents recorded from an individual oocyte coexpressing P2X4 and GluN2B-containing NMDARs responding to: Glutamate (Glu, 2 μM), ATP (5 μM), or Glu and ATP (2 μM and 5 μM respectively.) The predicted *additive* response (grey line) is calculated as the sum of the separate Glu and ATP induced currents. **(b)** Bar graphs comparing the predicted and actual responses obtained from coapplication of agonists for P2X4 and NMDARs containing GluN2A (n = 9), GluN2B (n = 9), or GluN2C (n = 10), normalized to the sum of the separate Glu and ATP responses for each oocyte. The data are expressed as mean ± SEM; Statistical analysis performed using paired t-test * $p< 0.05$, ** $p< 0.01$, *** $p< 0.001$, **** $p< 0.0001$. Similar results were seen using a saturating concentration of 100 mM Glu (data not shown).

2.1.2. Coactivation of P2X2 and NMDA receptors produces reciprocal inhibitory (cross-talk) responses

Given that both P2X2 and P2X4 are widely expressed in the CNS, we wanted to determine if P2X2 could also interact with NMDARs. In a similar manner, we coexpressed P2X2 and NMDARs in oocytes and recorded the currents evoked by application of ATP (100 μM), Glu (100 μM) or both agonists (100 μM each) (Figure 2). Similar to P2X4, P2X2 appeared to interact with NMDARs, as coactivation of P2X2 and NMDARs (containing GluN2A, GluN2B, or GluN2C) produced significantly lower responses than predicted (72.5±3.8 %, n = 21, $p< 0.0001$; 77.1±4.8 %,n = 22, $p< 0.0001$; 77.9±5.6 %, n = 6, $p< 0.05$, respectively). Unlike P2X4, NMDAR responses after P2X2 coactivation fully recovered (data not shown). Thus, to investigate the directional nature of this phenomenon, we added the agonists sequentially; i.e., ATP was coapplied when the Glu response reached its maximum or *vice versa* – Glu was coapplied when the ATP response reached its peak. As shown in Figure 2C, application of either ATP during Glu-evoked current or Glu during ATP-evoked current both led to responses that were significantly lower than the predicted sum of the individual responses. Collectively, these results suggest that P2X2 and NMDARs do not function in isolation and that an interaction leads to a functional and reciprocal cross-inhibition that is independent of the GluN2 subunits composition of the NMDARs.

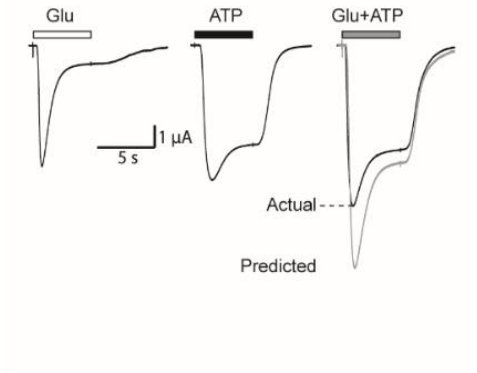

(a)

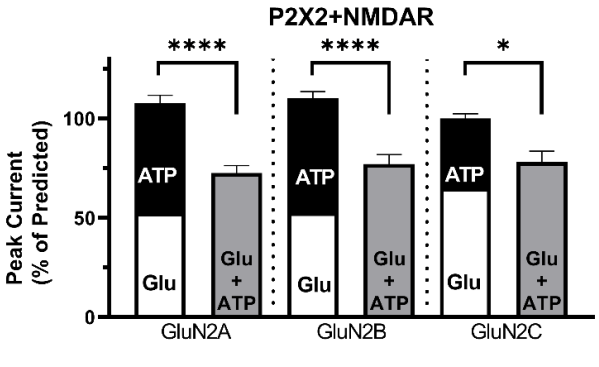

(b)

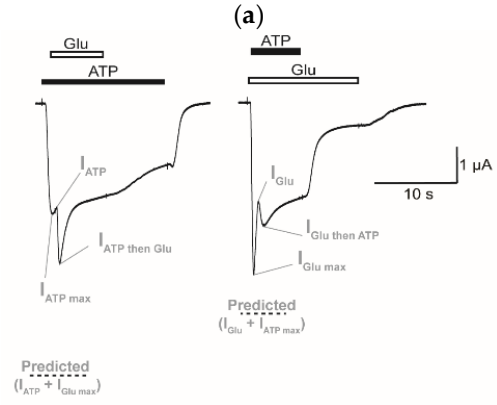

(c)

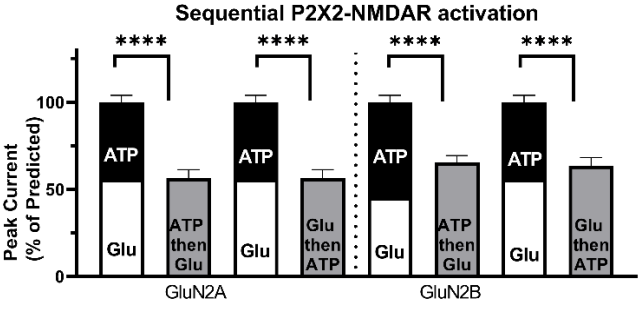

(d)

Figure 2. P2X2-NMDAR coactivation produces an inhibited response. **(a)** Representative current recorded from an individual oocyte coexpressing GluN2B-containing NMDARs and P2X2 responding to 100 μ*M*: Glu *(left)*, ATP (*middle)*, or Glu + ATP (right) are shown. **(b)** Bar graphs comparing the predicted and actual responses obtained from coapplication of agonists for P2X2 and NMDARs containing GluN2A (n = 22), GluN2B (n = 21), or GluN2C (n = 6), normalized to the sum of the separate Glu and ATP responses for each oocyte. **c)** Representative current from an individual oocyte coexpressing P2X2 and NMDARs containing GluN2B. For sequential activation of P2X2 and NMDARs, primary application of either ATP (left) or Glu (right) first appears to reduce subsequent coactivation responses. The predicted response when ATP is applied first is calculated as the sum of the current response to ATP immediately before Glu is coapplied and the maximum current response to Glu thereafter. This order is reversed when calculating the predicted response when Glu is applied first. **(d)** Bar graphs of P2X2 and GluN2A (n = 16) or GluN2B (n = 17) containing NMDARs, comparing the predicted and actual responses obtained from sequential activation and coapplication of agonists, normalized to the sum of the predicted current. The data are expressed as mean ± SEM; Statistical analysis performed using paired t-test * $p< 0.05$, ** $p< 0.01$, *** $p< 0.001$, **** $p< 0.0001$.

2.2. P2X4-NMDAR interactions are independent of Ca^{2+} influx

P2X4 and NMDAR both display a high calcium permeability [29] which raises the question of whether the inhibited responses observed during P2X4-NMDAR coactivation could be mediated by or depend on calcium. At the same time, the increased responses to Glu after P2X4-NMDAR coactivation may be explained by calcium influx via P2X4. Indeed, calcium influx has been shown to regulate NMDAR function, either by facilitating protein interactions [30] or activating downstream modulators [31, 32]. To determine whether the putative P2X4-NMDAR interaction was mediated by calcium influx, we utilized a Calcium-free Ringer's solution (CfRS) which substitutes barium chloride for the calcium chloride. In the absence of calcium, coactivation of P2X4 and NMDARs consistently produced significantly lower responses ($p< 0.0001$) than we predicted: P2X4 and GluN2A, GluN2B, and GluN2C produced 65.5 ±6.5 %, 48.2 ±5.4 %, and 85.7 ± 6.2 % of the predicted additive responses, respectively (Figure 3A). Additionally, the degree of inhibition was similar to if not greater than the inhibition obtained in Ca^{2+}-containing medium (Figure 1) indicating that the Ca^{2+}-influx through the opened receptor-channels does not mediate the observed inhibitory interaction between P2X4 and NMDARs. Furthermore, in the absence of calcium, we observed that the Glu responses by NMDARs containing GluN2B remained lower after coactivation with P2X4, again preventing the determination of the directional nature of this interaction.

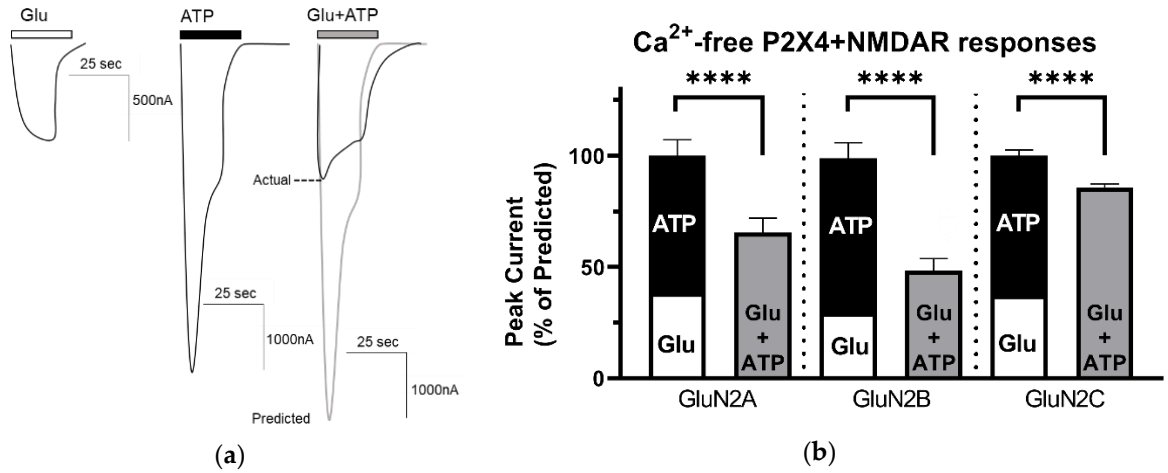

Figure 3. P2X4-NMDAR cross-talk is independent of calcium. (**a**) Representative currents recorded in Calcium-free Ringers' solution (CfRS) from an individual oocyte coexpressing P2X4 and GluN2B-containing NMDARs responding to: Glu (2 μM), ATP (5 μM), or Glu and ATP (2 μM and 5 μM respectively.) The predicted additive response (grey line) is calculated as the sum of the individual Glu and ATP induced currents.(**b**) Bar graphs representing the predicted and actual responses

obtained from coapplication of agonists, normalized to the sum of the separate Glu and ATP responses for each oocyte. For GluN2A, coactivation produced a statistically lower response than the predicted response ($p< 0.0001$; paired t-test; n = 10). The same result was observed for GluN2B ($p< 0.0001$; paired t-test; n = 9) and GluN2C ($p< 0.0001$; paired t-test; n = 28) coactivation. Furthermore, the degree of inhibition was not significantly different between the different GluN2 subunits (one-way ANOVA; $p>0.05$) The data are expressed as mean ± SEM; statistical analysis performed using paired t-test, * $p< 0.05$, ** $p< 0.01$, *** $p< 0.001$, **** $p< 0.0001$.

2.3 P2X4-induced a long-lasting inhibition of NMDAR is GluN2-subunit dependent

Activating P2X4 and NMDARs simultaneously (Figure 1) cannot inform the directionality of this interaction, as the effects of coactivation seem persistent. To further investigate the duration of P2X4-induced inhibition of NMDAR, we first obtained stable NMDAR currents by applying Glu every 5 min and recorded, after a single P2X4 mediated current evoked by application of ATP, Glu-evoked responses over the time, in the presence or absence of calcium (Figure 4). As shown in Figure 4A, the amplitude of GluN2B response in CfRS recorded 5 min after P2X4 activation was significantly lower than the one recorded before P2X4 activation, representing ~70% of the baseline response and seemed to recover only partially over time (Figure 4B). GluN2A and GluN2B showed similar reduced responses to Glu 5-min after P2X4 activation; 57.8 ± 6.6 % and 69.1 ± 4.04% of baseline, respectively. Consistent with the current inhibition observed during coapplication of both agonists (see Figures 1 and 3), NMDARs containing GluN2C showed the lowest effect-size 5 min after P2X4 activation with 87.5 ± 1.9 % of the baseline response to Glu. Recovery of the Glu responses over the time was distinct among the different GluN2 subunits. NMDARs containing GluN2A do not recover 15 min after P2X4 activation, with Glu-induced current representing 64.3 ± 5.0 % of the baseline responses to Glu. Similarly, GluN2C containing NMDARs, which showed the smallest effect size, behaved similarly after 15 min initial P2X4 activation, producing 87.3 ± 3.8 % of the

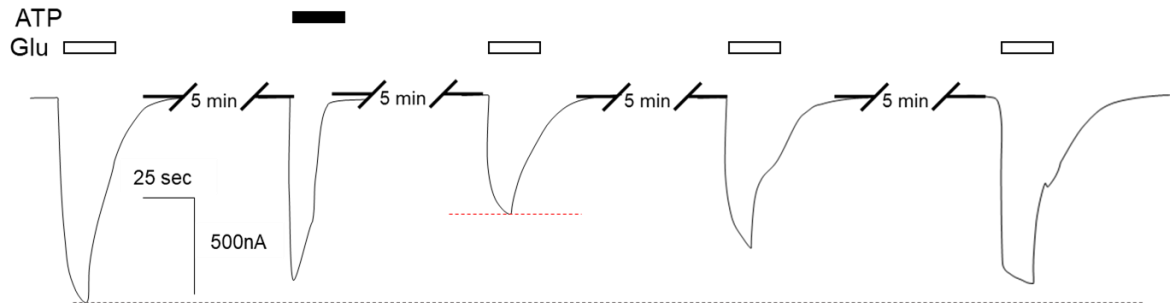

(**a**)

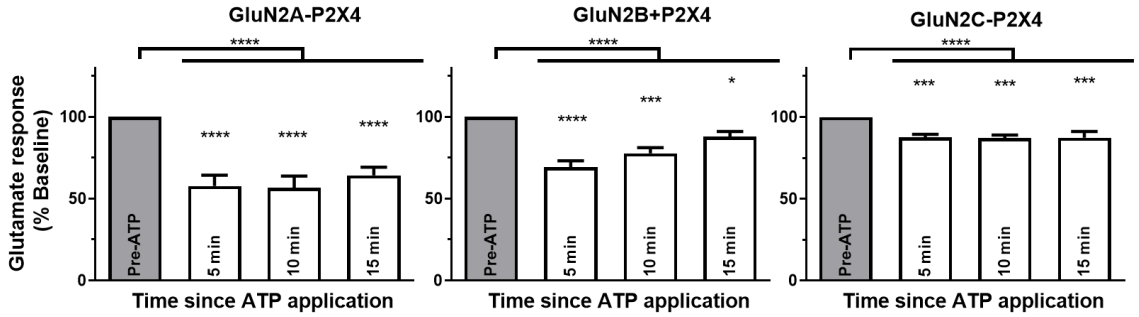

(**b**)

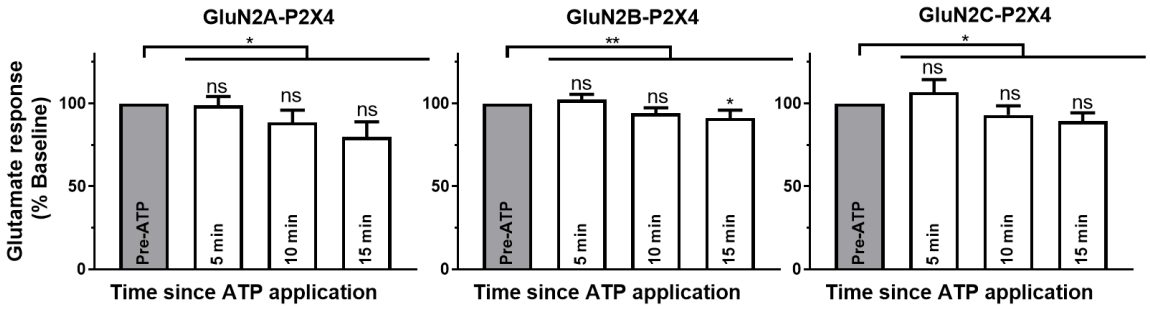

(c)

Figure 4. The time-course for recovery of P2X4-mediated NMDAR inhibition in the absence or presence of calcium. **(a)** Representative current evoked by application of Glu (2 μM), before and after activation of P2X4 by ATP (5 μM), from an individual oocyte coexpressing GluN2B-containing NMDARs and P2X4 in the absence of calcium (CfRS.) Bar graphs representing the mean of the amplitude of NMDARs responses in the absence **(b)** or presence **(c)** of calcium, before and after P2X4 activation by ATP. All values were normalized to the Glu response obtained before P2X4 stimulation. Glu responses after P2X4 activation were significantly lower NMDARs containing each of the GluN2A-C subunits in the absence of calcium (* $p< 0.05$, ** $p< 0.01$, *** $p< 0.001$, **** $p< 0.0001$, one-way ANOVA with Dunnet's post-hoc test; n=10-17 oocytes). Additionally, the time course of glutamate current recovery appears distinct, i.e. GluN2-subunit specific. The data are expressed as mean ± SEM. The same results are seen using a saturating concentration of 100 mM Glu (data not shown).

baseline responses to Glu. On the other hand, NMDARs containing GluN2B seemed to recover more rapidly, although 15 min after P2X4 activation, responses to Glu remained significantly inhibited ($p< 0.05$) representing 87.9 ± 3.1 % of the baseline response. Interestingly, while the presence of calcium (Figure 4C) produced significant differences between the NMDAR responses before and after P2X4 activation ($p< 0.05$), post-hoc analyses of Glu responses by GluN2A-C containing NMDARs were generally not significantly different from baseline ($p> 0.05$). Indeed, only GluN2B containing NMDARs showed a significant decrease in Glu responses, after 15 min. These results suggest that activation of P2X4 alone can induce a long-lasting inhibitory response from NMDARs, the extent and duration of which depends upon the nature of GluN2 subunit. These results also suggest that, while P2X4-NMDAR inhibitory interactions are independent of calcium influx, calcium entry via P2X4 can affect NMDAR function via a distinct mechanism.

2.4. Intracellular P2X domains mediate NMDAR interactions

Inhibitory forms of cross-talk were previously reported between several P2X subtypes and distinct members of the cys-loop receptor family (such as nicotinic receptors, $GABA_A$ or 5-HT3 receptors) which led to reciprocal or unilateral inhibition observed only during the coactivation of both receptors. These previous cross-talk investigations suggest (by mutagenesis, peptide competition, or domain overexpression experiments) that the phenomena rely on physical interactions between motifs within the C-terminal tail (CT) of P2X subunits and the intracellular loop between TM3 and TM4 of cys-loop receptors [17-23]. Since our results indicated that P2X2 and P2X4 could interact with NMDARs in a similar manner, we investigated whether the CT of these subunits is required for the interaction with NMDAR and whether a motif shared by both P2X subunit confer the ability to interact with NMDARs.

2.4.1 P2X-NMDAR inhibitory interactions depend on C-terminal P2X domains

We reasoned that if the mechanism of NMDAR inhibition relies on residues located in either P2X CT (see Figure 5A), then coexpressing the CT domain of P2X4 (K373-Q388; P2X4 CT) with P2X2 and

NMDAR would interfere and preclude inhibitory cross-talk between P2X2 and NMDAR. Reciprocally, expression of the CT domain of P2X2 (M3374-L472; P2X2 CT) should interfere with P2X4-NMDAR interactions and alter the previously inhibitory responses. As presented in Figure 5B, we found that the expression of a small construct (or minigene) encoding for only the P2X2 CT [17] in oocytes coexpressing P2X4 and GluN2A-containing NMDARs was capable of interfering with the GluN2A-P2X4 interaction, as the current inhibition observed between P2X4 and GluN2A (see Figure 1) during the coapplication of both agonists was abolished (104.9 ± 5.5 % of the predcition, $p > 0.05$.) Conversely, expression of a construct coding for P2X4 CT in oocytes coexpressing GluN2A containing NMDARs and P2X2 was able to abolish the functional cross-inhibition the interaction, as the coactivation response (96.2±3.9%) was not significantly different from the predicted sum of the individual responses ($p > 0.05$.). As a positive control, the expression of the P2X2 CT in oocytes coexpressing P2X2 and GluN2A-containing NMDARs abolished the cross-inhibition observed during P2X2-GluN2A coactivation (105.5±6.2% of the prediction, $p > 0.05$). These results suggest that neither P2X2 nor P2X4 interacted functionally with NMDAR in the presence of the CT domain of P2X2. These results also illustrate how cross-talk between P2X and NMDARs relies on the CT domain of P2X subunits. Overall, this work suggests that a common motif within the CT tail of P2X subunits can confer the ability to interact with NMDARs. To identify such motifs, we decided to perform mutagenesis analysis on the CT of P2X4, which is shorter (in amino acid length) than P2X2 subunits.

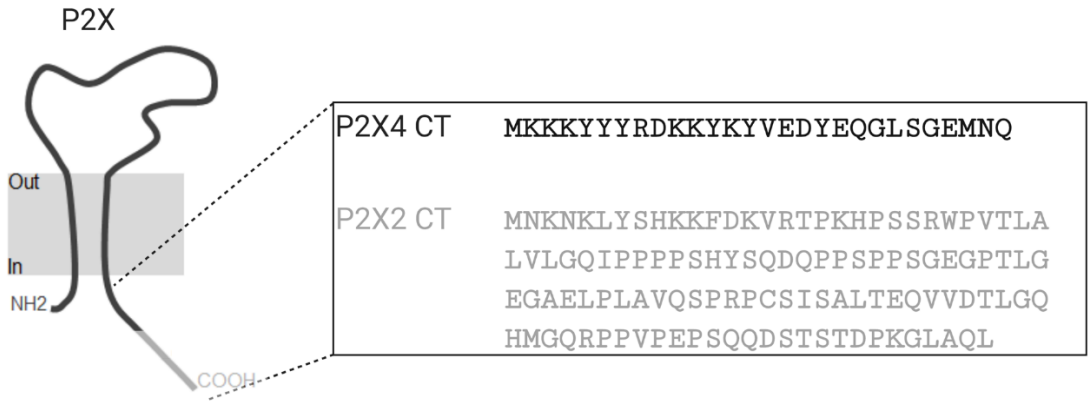

(**a**)

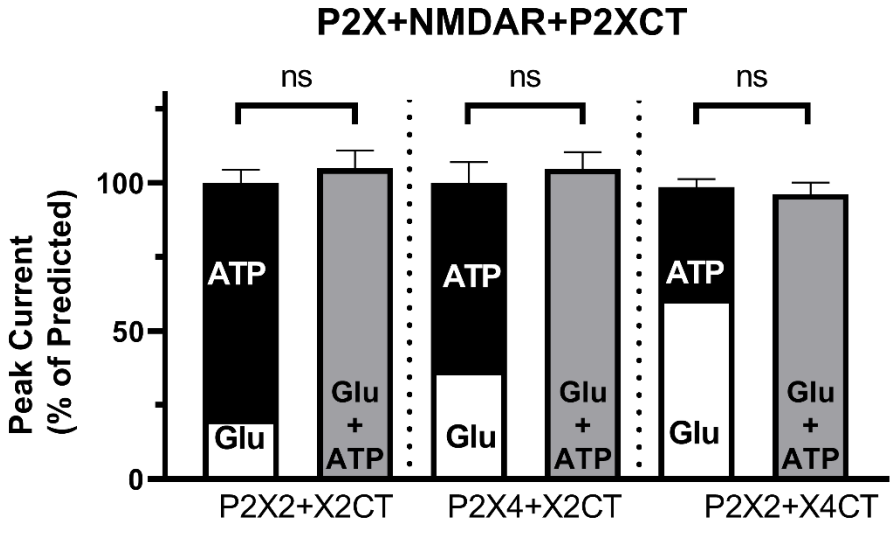

(**b**)

Figure 5. P2X CT mediate interactions with NMDARs. (**a**) *Top* A representative illustration of a homotrimeric P2X. The insert illustrates the differences in the size of the P2X4 (black) and P2X2 (grey) CT. (**b**) Bar graphs representing the predicted and actual responses obtained from coapplication of Glu (2 μM) and ATP (5 μM) in oocytes expressing either the P2X2 CT or the P2X4 CT, in combination with P2X2s or P2X4s and NMDARs. Agonist responses were normalized to the sum of the individual Glu and ATP responses for each oocyte. There was no statistically significant difference between the predicted responses and the actual responses produced by GluN2A-containing NMDARs and P2X4s in the presence of the P2X2 CT (105.0±5.5% , p> 0.05, n=7) Similarly, there was no statistically significant difference between the predicted responses and the actual responses produced GluN2A-containing NMDARs and P2X2s in the presence of the P2X4 CT (96.2±3.9% , p> 0.05, n=10) or the P2X2 CT (106.0±6.21% , p> 0.05, n=2). The data are expressed as mean ± SEM. Statistical analysis performed using paired t-test.

2.4.2 Resolving the P2X4 CT domain responsible for NMDAR inhibition

Among the seven P2X subunits, P2X4 is the only subunit to rely on a non-canonical motif (Y_{378}XXGL_{382}) of endocytosis [33, 34] to undergo constitutive internalization. It is important to note that previously, GABA-P2X4 cross-talk was shown to be independent of this domain, relying instead on two other CT residues: Y_{374} and V_{375} [20]. To investigate whether the residues in the P2X4 CT that are responsible for P2X4 internalization are also responsible for the interaction with NMDARs, we truncated or replaced the P2X4 internalization motif, as illustrated in Figure 6A. We hypothesized that, if residues in the internalization domain of P2X4 are responsible for mediating NMDAR inhibition, then truncating the P2X4 receptor at residue 377 (P2X4-377TR) or replacing the internalization domain (YEQGL) of the wildtype P2X4 receptor with a FLAG epitope (DYKDDDK; P2X4-FlagIN) would abolish the inhibitory effects of receptor costimulation. Similarly, if only the internalization motif were driving the interaction with NMDARs, then truncating P2X4 after the internalization motif, corresponding to residue 382, (P2X4-382TR) would still show inhibitory coactivation responses. Figure 6B shows that the inhibitory response previously shown (i.e., Figure 2) were no longer present when coactivating either P2X4-377TR or P2X4-FlagIN. Furthermore, Figure A3 shows that P2X4-377TR failed to produce the long-lasting inhibition previously seen by full-length P2X4 in the absence of calcium, as shown in Figure 4B. Unexpectedly, we did not see any inhibitory P2X4-NMDAR coactivation responses when P2X4s were truncated at residue 382, (P2X4-382TR) despite the inclusion of the P2X4 internalization motif in these mutant receptors. Collectively, these results suggest that the distal part of the CT tail, corresponding to the last 11 amino-acids of P2X4, is necessary for P2X4 to functionally interact with NMDARs.

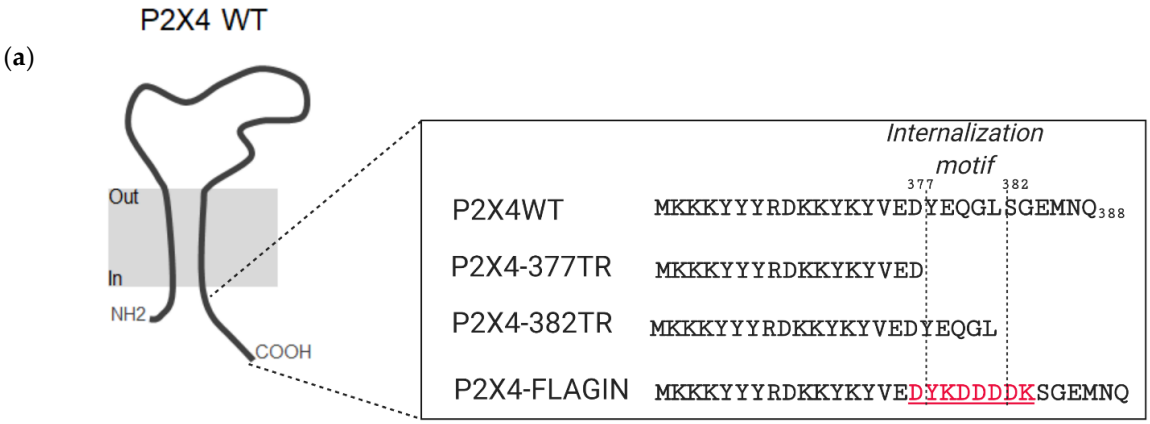

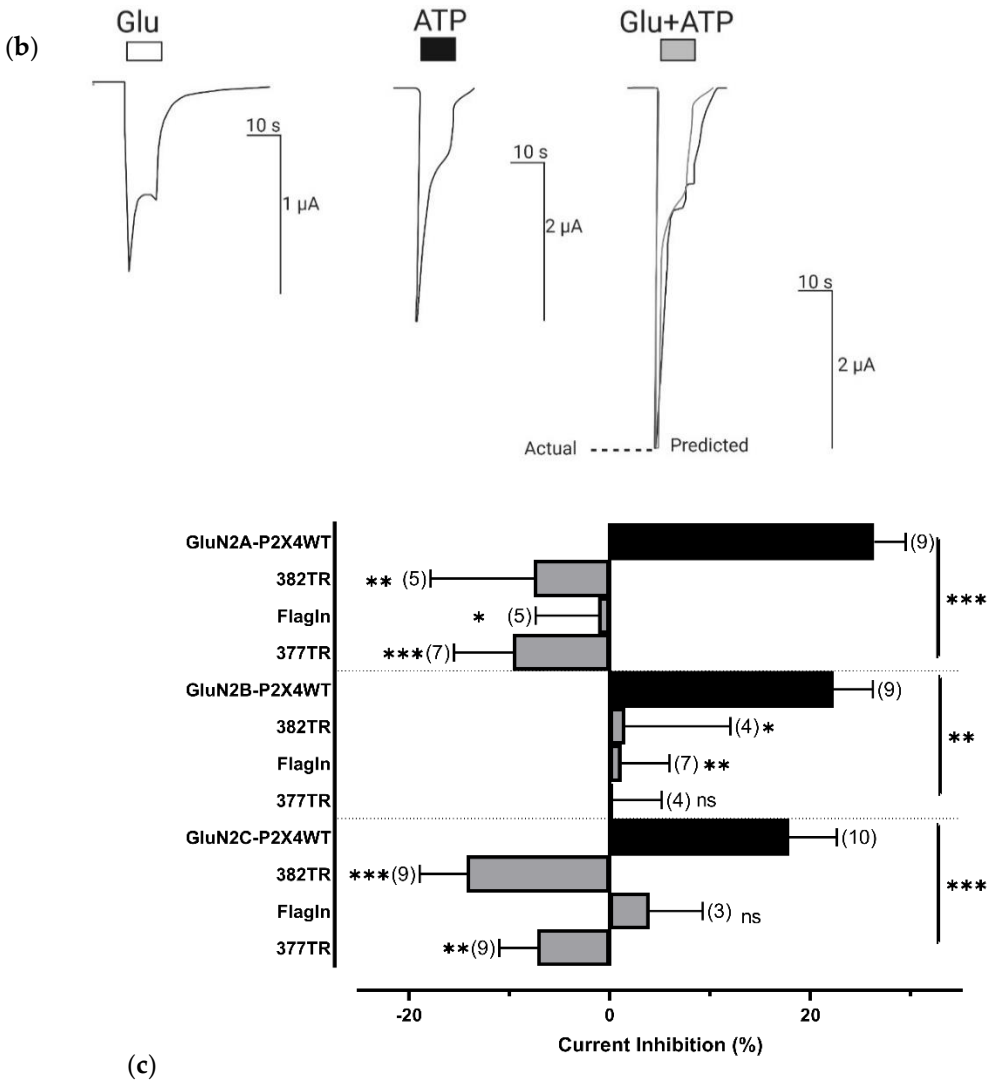

Figure 6. Residues in the P2X4 CT confer the ability to interact with NMDARs. (**a**) An illustration of the mutations performed on the P2X4 internalization motif, compared to the wildtype P2X4 (P2X4WT); (**b**) Representative currents recorded in Ringers' solution from an individual oocyte coexpressing P2X4-377TR and GluN2A-containing NMDARs responding to: Glu (2 μM), ATP (1 μM), or Glu and ATP (2 μM and 1 μM respectively.) The predicted additive response (grey line) is calculated as the sum of the individual Glu and ATP induced currents. (**c**) Bar graphs representing the current inhibition obtained from coapplication of Glu and ATP for oocytes coexpressing different P2X4 mutants and NMDARs. Agonist responses were normalized to the sum of the individual Glu and ATP responses for each oocyte and subtracted from 100%. The data are expressed as mean ± SEM. P2X4 CT mutations were statistically significantly different ($p< 0.05$) from the previously obtained inhibitory coactivation responses for each GluN2 subunit (Kruskal-Wallis test with Dunn's post-hoc analysis.) *ns*>0.05, * $p< 0.05$, ** $p< 0.01$, *** $p< 0.001$, **** $p< 0.0001$ Parentheses denote number of replicates.

2.4.3 A small peptide disrupts P2X-NMDAR interactions

Recombinant studies have shown that a peptide corresponding to the last 11 amino-acids of P2X4 subunit (namely 11C) blocks P2X4 internalization and was previously used to determine the function of increased surface P2X4 in neurons from hypothalamus brain slices [20]. To confirm whether the distal domain of P2X4 is necessary and sufficient to ablate inhibitory cross-talk with NMDARs, we reproduced the interaction-competition experiments as described in Figure 5, but instead of

coexpressing the P2X4 CT, we injected the 11C peptide into oocytes (150 μM final concentration) expressing P2X2 or P2X4 in combination with NMDARs containing GluN2A, GluN2B, or GluN2C. Figure 7 showed that the presence of peptide 11C abolished the observed inhibitory responses during the coactivation of both receptor types (see Figure 2B and 2D.)

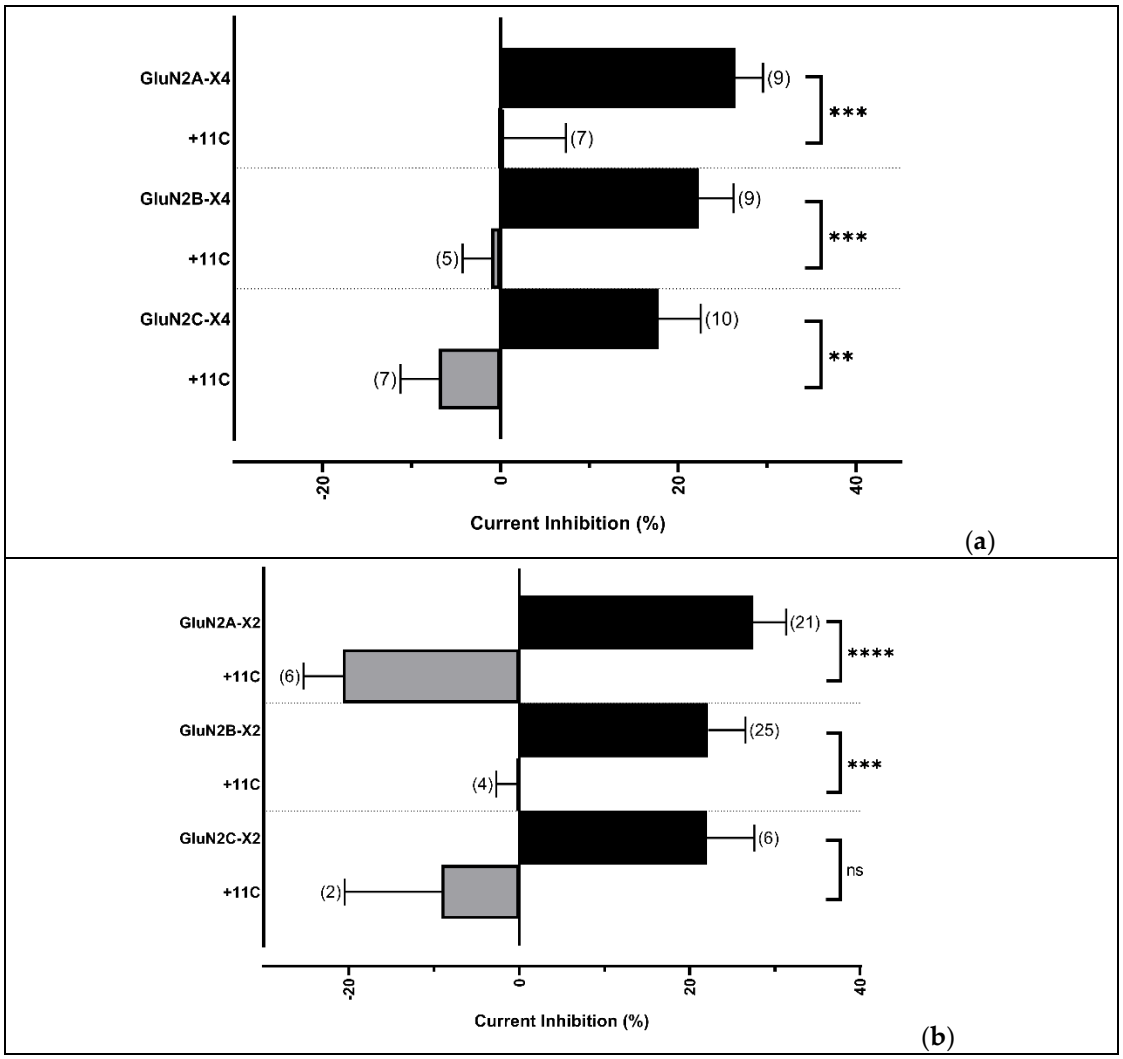

Figure 7. 11C peptide disrupts P2X-NMDAR cross-talk. Bar graphs representing the current inhibition obtained from coapplication of Glu and ATP for oocytes expressing either P2X4 (**a**) or P2X2 (**b**) and NMDARs containing GluN2A-C, 30 minutes after injection with 11C (grey). The inhibitory responses (black) are ablated by 11C. Agonist responses were normalized to the sum of the individual Glu and ATP responses for each oocyte and subtracted from 100%. The data are expressed as mean ± SEM and were analyzed using a Welch's *t*-test. *ns*>0.05, * p< 0.05, ** p< 0.01, *** p< 0.001, **** p< 0.0001 Parentheses denote number of replicates.

3. Discussion

P2X modulation of NMDA receptors

Our results are the first to provide direct evidence for and characterize P2X-NMDA interactions. We found that, when heterologously expressed in *Xenopus laevis* oocytes, P2X4 can interact with and inhibit NMDAR function consisting of GluN2A-C subunits (Figure 1) Furthermore, we report a similar inhibitory phenomenon between P2X2 and NMDA receptors (Figure 2) Interestingly, this P2X2-NMDA receptor interaction seems to be reciprocal in nature (each receptor inhibits the other; *cross-talk*.) These results indicate that P2X modulation of NMDARs may be more complicated and robust than the early reports [7, 8, 35].

Our results support the hypothesis that P2X serve an important role in modulating the function of NMDARs and provide new context for which to interpret the function of P2Xs; this has remained elusive, if not controversial. Early studies reported that P2X could contribute to synaptic transmission, albeit sparsely, and suggested that P2X could function as a "low-frequency filter", suppressing NMDAR-mediated LTP under weak stimuli [35]. With the development of P2X4 KO mice came more support for a role for P2Xs in synaptic plasticity: 1) in the absence of P2X4, hippocampal neurons exhibited reduced LTP facilitation, and 2) Ivermectin, a P2X4 positive allosteric modulator, could increase LTP in wildtype mice, but not P2X4 KO mice [6]. These results suggested that P2X in the post-synaptic membrane modulate NMDAR function and LTP induction via calcium influx, rather than through synaptic transmission. However, studies have also demonstrated that P2X4 themselves must contribute to NMDAR modulation at post-synaptic densities, as intracellular administration of a calcium chelator could block NMDAR facilitation in WT mice, but had no effect in P2X4 KO mice. [7]. Indeed, our results indicate that these hypotheses regarding the mechanism of P2X modulation of NMDARs are not mutually exclusive, as we found that Calcium-free Ringer's solution did not preclude P2X4-NMDAR cross-talk during receptor coactivation (Figure 3A) but that, in the presence of calcium, Glu responses by NMDARs after P2X4-NMDAR coactivation increase (Figure 1C). Collectively, our results suggest that, while the interaction between P2X4 and NMDARs may be long-lasting, calcium influx via P2X4 plays a distinct role in modulating NMDARs.

Until recently, the modulatory nature of P2Xs (including regulation of NMDARs) was inextricably linked to their ability to permeate calcium. However, with the characterization of a novel knock-in mouse strain, where P2X4 is fluorescently labeled and internalization-deficient (P2X4mCherryIn), a more nuanced role for P2X has emerged [15]. The study demonstrated that in CA1 synapses, P2X4mCherryIn mice displayed no changes in basal excitatory transmission, but exhibit changes to LTP and LTD induction. Considering that, in CA1 hippocampus neurons, LTP and LTD have been shown to rely on post-synaptic NMDARs [36] (for review on LTP see[37]), these results suggest that increased P2X4 activity in CA1 neurons alters NMDAR function, supporting the idea that P2X4s are involved in regulating synaptic plasticity.

P2X intracellular domains mediate NMDAR cross-talk

Interactions of P2X2 and P2X4 were demonstrated for nicotinic [21], GABA [18], AMPA [27], and 5-HT_{3A} receptors [22, 23]. This P2X-mediated regulation of other LGICs has been found to rely on diverse mechanisms 1) physical protein-protein interactions, 2) receptor cotrafficking, or 3) signaling cascades, which can all be linked to direct interactions involving the receptor CT. P2X2 are similar in sequence and structure to P2X4, with the most prominent differences being found between the intracellular CTs. In an effort to better understand the receptor domains that drive this interaction, we chose to focus on the P2X4 CT, which is significantly shorter and thus more simple to mutate [33, 38]. Our studies show that truncation of P2X4 before the start of their internalization motif ablated NMDAR cross-talk, which leads one to believe that this interaction might be dependent upon P2X4 trafficking. Replacing only the internalization motif (YEQGL) with a flag epitope (DYKDDDKD) also ablated cross-talk, which seemed to confirm the significance of the domain. However, the P2X4 internalization motif does not seem to mediate this interaction entirely, as P2X4 truncated after the internalization motif also fail to interact with NMDARs (Figure 6). In support of this notion, the well characterized non-canonical tyrosine-based sorting motif *YXXGL* [33, 34] [38], was not shown to be responsible for the cross-talk interaction between P2X4 and GABA receptors [20]

While this resolves the interaction between P2X4 and NMDARs, does P2X2 interact with NMDARs via a similar mechanism? Based on the P2X4 truncation results, we reasoned that, if the P2X2 and P2X4 CT did mediate interactions with NMDA receptors, coexpressing the P2X4 CT in oocytes would interfere with P2X2-NMDAR cross-talk, and vice versa. As shown in Figure 5, our results are consistent with the hypothesis that each CT disrupted the inhibitory responses that we presented in Figures 1 and 2. Our mutation investigations suggested that the distal 11 CT residues of P2X4 seem

to be required for NMDAR interaction, allowing us to hypothesize that suppression of cross-talk could be achieved by a peptide mimicking this domain. We synthesized and injected 11C as reported [20], and found that 11C ablated P2X2 and P2X4 interactions with NMDARs, suggesting that this interaction relies on several key residues found on the intracellular domains of P2X. Given that P2X2-NMDAR cross-talk was suppressed by 11C, our results also suggest that P2X2-NMDAR interactions rely on similar residues.

How could the CT of both P2X4 and P2X2 mediate inhibition of NMDA receptors, given the size difference of these domains? Studies on the P2X4 CT and its non-canonical internalization motif revealed that, when co-crystalized with the μ2 AP subunit, residues 374 to 380 do not adopt a rigid structure [34]. Furthermore, the non-canonical YXXGL motif functions at the same canonical YXXΦ site due to the flexibility imparted by the glycine residue. When looking at the composition of the P2X2 CT, proline and other hydrophobic residues are prevalent. This is notable because proline can disrupt secondary protein structures and limit flexibility, while hydrophobic residues can promote a more "buried" conformation. It is possible that these residues allow the P2X2 CT to adopt a conformation that favors an interaction with NMDA receptors, much like in the case with P2X4. Unfortunately, no structural information exists for the P2X2 CT, which would provide more insight into their function. Despite these limitations, future studies can investigate the GluN2 region responsible for this P2X interaction, as well as the exact residues mediate P2X-NMDAR cross-talk, using a point-mutation approach.

Resolving the function of P2X in the brain

Distinct forms of P2X cross-talk might serve discrete regulatory functions and arise from P2X mobility and localization, which has been shown to be subunit dependent. For example, P2X2 are highly mobile and stable at the cell surface, but rarely found on synaptic densities [39, 40]. On the other hand, P2X4 are primarily found within intracellular compartments (due to constitutive internalization). Evidence has already shown that P2X4 play a role in integrating ATP signaling from astrocytes in the tripartite synapse, specifically by inhibiting GluN2B-containing NMDARs, an interaction that involves a multiprotein complex [8]. As such, P2X2 at extra synaptic densities may serve as molecular "trap", inhibiting NMDAs via an interaction that prevents their inclusion into the post-synaptic densities. The reciprocal nature of this interaction might act as a negative feedback loop and allow for more diverse responses or fine tuning. In contrast, P2X4s can act in a more targeted manner, waiting inside the cell and mobilizing into the post-synaptic density when stimulated.

4. Materials and Methods

Molecular Biology

Rat GluN receptor subunits were a kind gift from Dr. John Woodward. P2X4 cDNA was a kind gift from Dr. Iain Chessell and GlaxoSmithKline, and cloned into the pCDNA3.1 vector as previously described [41] while P2X2 cDNA was cloned into pCDNA3 [17]). pUNIV backbone was a gift from Cynthia Czajkowski (Addgene plasmid # 24705 ; http://n2t.net/addgene:24705 ; RRID:Addgene_24705) and was modified for subcloning of rat GluN subunits (to enhance RNA expression.) Mutant receptors (P2X4 377-TR, P2X4-FlagIn) or P2X-CT minigenes were either available from previous studies [17-20, 38] or mutated using the SuperFi PCR kit and transformed into Zymo Mix&Go competent cells. Single colonies were inoculated into Luria Broth and after 16-20 hours, minipreps were performed using the ZymoPure miniprep kit. Plasmids were then restriction-digested with NotI-HF (New England Biolabs) and purified using the Zymo DNA clean-up kit. All constructs were sequence verified via sanger sequencing (Genewiz; La Jolla,CA). The 11C peptide was synthesized by GenScript (Piscataway, NJ, USA), reconstituted (110mM) in ultrapure water, and diluted to 10 mM using HEPES (10 mM; pH 7.2). Single-use aliquots were stored in -20°C prior to injection.

Xenopus laevis Oocyte injection and electrophysiology

cRNA for experiments were synthesized with the Ambion message machine T7 kit (ThermoFisher Scientific), purified using the Ambion MegaClear kit (ThermoFisher Scientific), and injected into *Xenopus laevis* oocytes (Ecocyte Biosciences, Austin, TX). Previous studies have reported functional receptors using an injection concentration of approximately 10 ng of total NMDA RNA (5 ng of GluN1 and 5 ng of GluN2 subunit), 10-20pg of P2X2 RNA, or 20 ng of P2X4 receptor RNA. 10-20ng P2X4 RNA or 5-10ng of NMDAR RNA was injected alone or combined, with a final injection volume of 40 nL. For P2X2 studies, 10-20pg of P2X2 RNA or 0.25-1ng of total NMDAR RNA was injected alone or combined and injected into each cell, with a final injection volume of 40 nL. 11C peptide injections were performed 30 minutes before TEVC recordings. 15 nL of 10 mM 11C peptide in HEPES was injected into each oocyte, for an approximate intracellular concentration of 150 μM. 1ng of CT minigenes were injected into oocytes in an injection volume of 20 nL, with injections performed 1 day before recordings. All injections were performed using a NanoJect III system (Drummond). Recordings were performed 1-3 days after cRNA injection. Two-electrode voltage clamp recordings were performed using previously established methods [41, 42]. In brief, oocyte membrane potentials were clamped at -70 mV using oocyte clamp OC-725C (Warner Instruments, Hamden, CT), and the oocyte recording chamber was continuously perfused with Ringer's solution ± agonist using a Dynamax peristaltic pump (Rainin Instrument Co., Emeryville, CA) at 3 ml/min using an 18-gauge polyethylene tube (Becton Dickinson, Sparks, MD). All perfusion solutions contain a buffer solution consisting of 115mM NaCl, 2.5mM KCl, 1.8mM $CaCl_2$ (or 1.8 mM $BaCl_2$ to avoid calcium induced current generated by Ringer's solution), and 10mM 4-(2-hydroxyethyl)-1-piperazineethanesulfonic acid (HEPES), with a final pH of 7.2. In the presence of calcium, Glutamate and/or ATP were applied for 10 seconds (to reach a peak current response). In the absence of calcium, (i.e. Calcium-free Ringer's solution or CfRS) Glutamate and/or ATP were applied for 25 seconds. A wait time of at least 5 minutes of perfusion buffer occurred between any agonist applications as to ensure complete washout of agonist. The resulting currents were filtered at 5kHz and recorded using an analog chart recorder (Linear). All current values obtained were normalized to the most recent stable responses obtained immediately before agonist coapplications began, unless stated otherwise. Figures were created with BioRender.com

Data Analysis.

Data were obtained from several batches of oocytes from at least three different frogs, and are expressed as mean ±S.E.M. The effects of costimulation are presented as percentages of the stable currents evoked by ATP and glutamate alone on individual oocytes, or as a percentage of the inhibition previously observed. The Prism 8 software suite (GraphPad Software, Inc., San Diego, CA) was used for data analysis and curve fitting. Statistical analysis was performed using student's paired t-test, Welch's t-test, one-way ANOVA followed by a Bonferroni post-hoc comparison, or Kruskal-Wallis test with a Dunn's test for multiple comparisons, as noted. Significance was set at $p < 0.05$.

Author Contributions: Conceptualization, L.R., L.A., E.B-G., and D.D.; methodology, L.R., E.B-G., L.A., and D.D.; validation, L.R. and E.B-G.; formal analysis, L.R., E.B-G., and Q.D.; investigation, L.R., C.Y., C.C., Q.D., S.W., M.R., and B.R.; resources, D.D. and E. B-G.; data curation, L.R., E.B-G., C.Y., C.C., Q.D., S.W., M.R., B.R.; writing—original draft preparation, L.R., L.A., E.B-G., D.D., C.Y., C.C., Q.D., S.W., M.R., and B.R.; writing—review and editing, L.R., L.A., E.B-G., and D.D.; visualization, L.R. and L.A.; supervision, L.R., L.A., E.B-G., and D.D.; project administration, L.R. and D.D.; funding acquisition, D.D., E. B-G., and L.R. All authors have read and agreed to the published version of the manuscript.

Funding: This work was supported by funding and grants from the NIH NIAA R01AA022448 (D.D.) and a diversity supplement (L.R.) to this grant as well as from the American Foundation for Pharmaceutical Education Pre-doctoral fellowship (L.R.), USC Undergraduate research Fund (D.D.), USC Good Neighbors Campaign (D.D.), and the USC School of Pharmacy. Funding support was also provided from CNRS and university of Bordeaux (E.B-G.) **Acknowledgments:** We would like to thank Albert Lam, and Audrey Martinez for their technical assistance during this project, as well as Jesse Chen, Tahmina Hasan, Ed Jeong, Alan Guan, Istiak Aziz,

and Nirali Patel for their assistance in collecting data. We would also like to thank Dr. John Woodward for his kind gift of plasmids containing the GluN subunits.

Conflicts of Interest: The authors declare no conflict of interest. The funders had no role in the design of the study; in the collection, analyses, or interpretation of data; in the writing of the manuscript, or in the decision to publish the results.

Abbreviations

P2X	Purinergic receptors
NMDARs	N-methyl-D-aspartate receptors
GABA	γ-aminobutyric acid
AMPA	α-amino-3-hydroxy-5- methyl-4-isoxazolepropionic acid
CT	Carboxy-terminal tail
LGICS	Ligand-gated ion channels
ATP	Adenosine triphosphate
CNS	Central nervous system
P2X4 KO	P2X4 knockout
LTP	Long-term potentiation
LTD	Long-term depression
TEVC	Two-electrode voltage clamp
Glu	Glutamate
CfRS	Calcium-free Ringers' solution
P2X4-377TR	P2X4 receptor truncated at residue 377
P2X4-382TR	P2X4 receptor truncated at residue 382
P2X4-FlagIN	P2X4 receptor with a FLAG epitope in place of internalization domain (YEQGL)
11C	Peptide consisting of the distal C-terminal 11 amino-acids of P2X4
5-HT_{3A}	5-Hydroxytryptamine Receptor 3A

Appendix A

To evaluate the potential functional interaction between P2X and NMDARs using two-electrode voltage-clamp (TEVC) we coexpressed both receptor types in *Xenopus laevis* oocytes. We performed mRNA injection of P2X or NMDARs at previously reported concentrations, titrating injections until each receptor system produced comparable currents. We then generated 8-point concentration response curves for oocytes expressing either P2X4 or NMDARs (GluN1 and GluN2A or GluN2B or GluN2C). The EC_{50} values for P2X4 and NMDA receptors calculated from ATP and Glu concentration response curves (Figure A1a-d, solid lines), were consistent with previously reported values [38, 43]. We then generated an 8-point ATP or Glu concentration response curve for oocytes coexpressing both P2Xs and NMDARs. There were no shifts in concentration response curves when P2X4s and NMDARs were coexpressed (Fig. 1a-d, dotted lines vs solid lines). Consistently, there were no statistically significant differences in the EC50 values for receptors regardless those were expressing individually or in combination (Figure A1). These studies demonstrate that coexpressing both P2X and NMDARs does not change the function of either receptor.

Appendix B

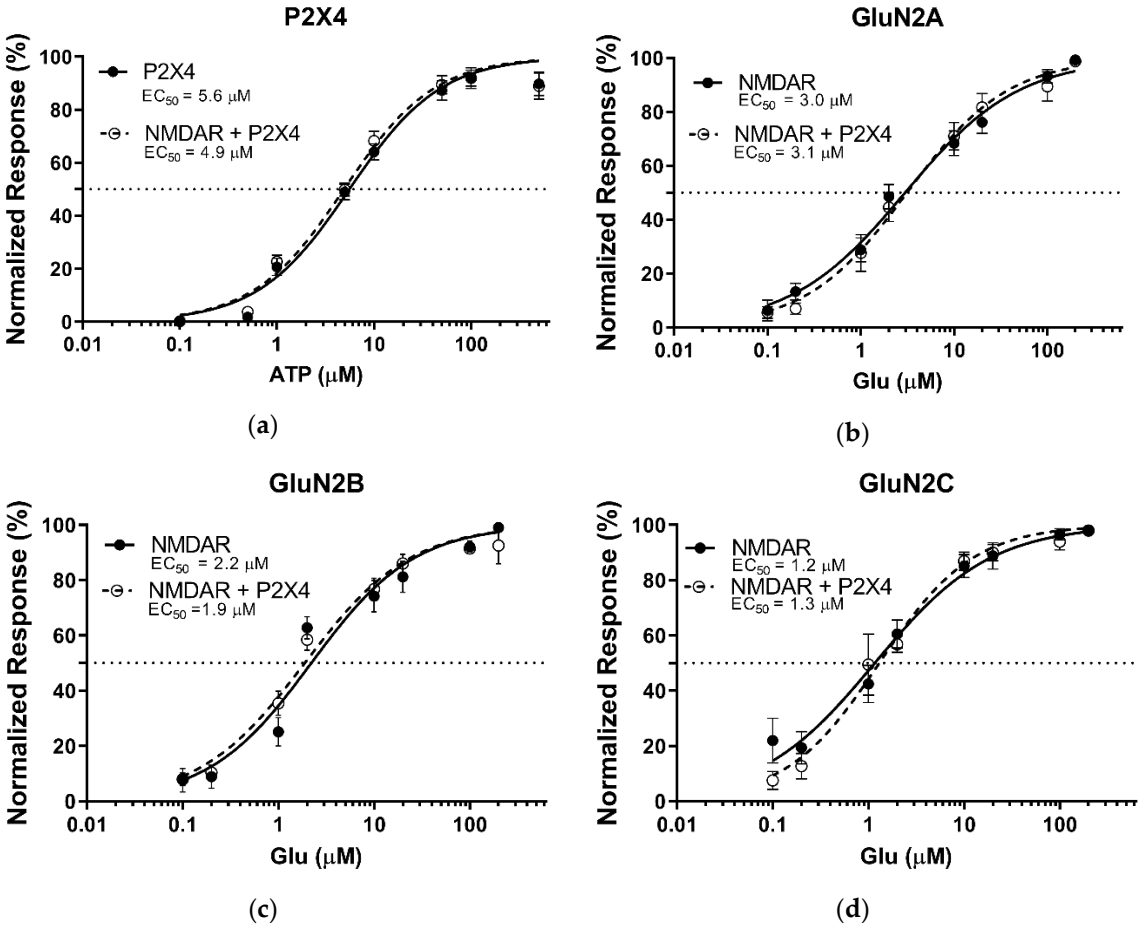

Figure A1. Comparison of the concentration-response curves for P2X4Rs or NMDARs expressed individually (depicted with solid lines) or together (depicted with dotted lines) in *Xenopus* oocytes. **(a)** ATP concentration-response curves. EC_{50} values obtained from ATP-concentration curves of individual P2X4 and P2X4 coexpressed with NMDARs were not significantly different. **(b-d)** Glutamate-concentration response curves. EC_{50} values were not statistically significantly different for Glu-concentration response curves for individual GluN2A, GluN2B, GluN2C (solid lines) and each NMDAR subtype coexpressed with P2X4 (dotted lines). P2X4 and NMDARs were injected at respectively 20 ng and 10 ng cRNAs. Data represent Mean ± SEM. Statistical analysis performed using Exact sum-of-squares F-test. **(a)** $p > 0.5$; n=9-12; **(b)** $p > 0.5$; n=9-12; **(c)** $p > 0.3$; n=9-12; **(d)** $p > 0.5$; n=9-12.

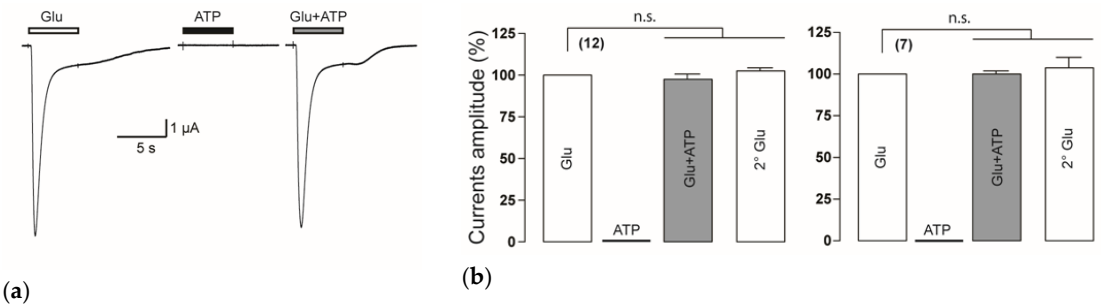

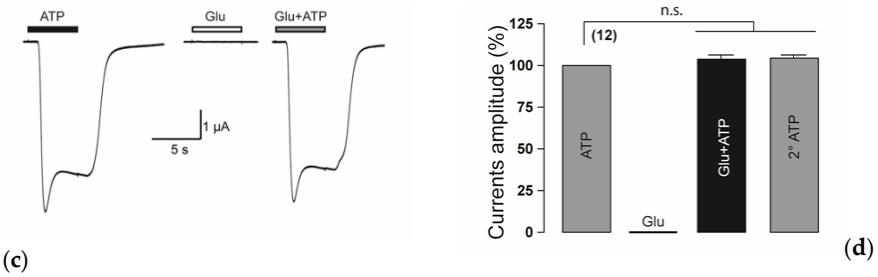

Figure A2. Application of ATP agonist does not affect Glu responses when NMDARs are expressed alone and conversely, application of Glu does not modulate ATP responses when P2X are expressed alone. **(a)** Representative current recorded from an individual oocyte GluN2B-containing NMDARs responding to 100 µ*M*: Glu *(left)*, ATP (*middle)*, or Glu + ATP (right) are shown.; **(b)** Bar graphs representing the current obtained from application of agonists, normalized to the Glu response for each GluN2B-expressing oocyte.; **(c)** Representative current recorded from an individual oocyte expressing only P2X2 responding to 100 µ*M*: ATP *(left)*, Glu (*middle)*, or Glu + ATP (right) are shown. **(d)** Bar graphs representing the current obtained from application of agonists, normalized to the ATP response for each P2X2-expressing oocyte. The data are expressed as mean ± SEM. *ns*>0.05 (one-way ANOVA)

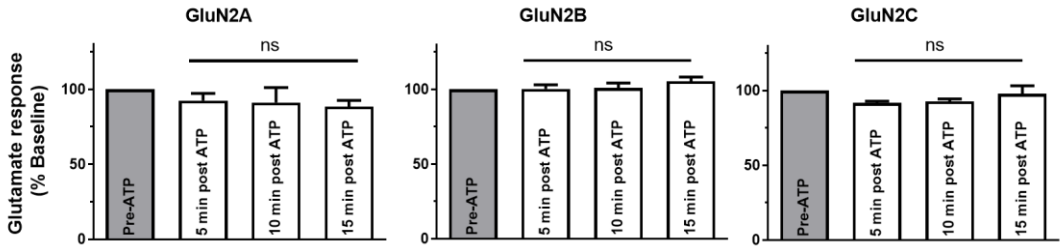

Figure A3. P2X4-mediated NMDAR inhibition depends on the P2X4 CT domain. Bar graphs representing the mean of the amplitude of NMDARs responses in CfRS before and after P2X4-377TR activation by ATP. All values were normalized to the Glu response obtained before P2X4-377TR stimulation. None of the Glu responses after ATP application were statistically significantly different (p> 0.05) from the baseline response (before ATP application) for any GluN2 subunit. The data are expressed as mean ± SEM. Statistical analysis performed using a one-way ANOVA test.

References

1. Barria, A. and R. Malinow, *Subunit-Specific NMDA Receptor Trafficking to Synapses.* Neuron, 2002. **35**(2): p. 345-353.
2. Kopec, C.D., et al., *Glutamate receptor exocytosis and spine enlargement during chemically induced long-term potentiation.* J Neurosci, 2006. **26**(7): p. 2000-9.

3. Khakh, Baljit S. and R.A. North, *Neuromodulation by Extracellular ATP and P2X Receptors in the CNS.* Neuron, 2012. **76**(1): p. 51-69.
4. Mori, M., et al., *Fast synaptic transmission mediated by P2X receptors in CA3 pyramidal cells of rat hippocampal slice cultures.* J Physiol, 2001. **535**(Pt 1): p. 115-23.
5. Jo, Y.H. and R. Schlichter, *Synaptic corelease of ATP and GABA in cultured spinal neurons.* Nat Neurosci, 1999. **2**(3): p. 241-5.
6. Sim, J.A., et al., *Altered Hippocampal Synaptic Potentiation in P2X4 Knock-Out Mice.* The Journal of Neuroscience, 2006. **26**(35): p. 9006-9009.
7. Baxter, A.W., et al., *Role of P2X4 receptors in synaptic strengthening in mouse CA1 hippocampal neurons.* European Journal of Neuroscience, 2011. **34**(2): p. 213-220.
8. Lalo, U., et al., *ATP from synaptic terminals and astrocytes regulates NMDA receptors and synaptic plasticity through PSD-95 multi-protein complex*. 2016. **6**: p. 33609.
9. Wyatt, L.R., et al., *Contribution of P2X4 receptors to ethanol intake in male C57BL/6 mice.* Neurochemical research, 2014. **39**(6): p. 1127-1139.
10. Wyatt, L.R.G., Sean C; Khoja, Sheraz; Jakowec, Michael W; Alkana, Ronald L; Bortolato, Marco; and Davies, Daryl L, *Sociocommunicative and Sensorimotor Impairments in Male P2X4-Deficient Mice.* Neuropsychopharmacology, 2013. **38**: p. 10.
11. Khoja, S.S., Vivek; Garcia, Damaris; Asatryan, Liana; Jakowec, Michael W.; and Davies, Daryl L, *Role of purinergic P2X4 receptors in regulating striatal dopamine homeostasis and dependent behaviors.* Journal of Neurochemistry, 2016. **139**(1): p. 14.
12. Stokes, L., et al., *To Inhibit or Enhance? Is There a Benefit to Positive Allosteric Modulation of P2X Receptors?* Frontiers in Pharmacology, 2020. **11**(627).
13. Yardley, M.M., et al., *Ivermectin reduces alcohol intake and preference in mice.* Neuropharmacology, 2012. **63**(2): p. 190-201.
14. Huynh, N., et al., *Preclinical development of moxidectin as a novel therapeutic for alcohol use disorder.* Neuropharmacology, 2017. **113, Part A**: p. 60-70.
15. Bertin, E., et al., *Increased surface P2X4 receptor regulates anxiety and memory in P2X4 internalization-defective knock-in mice.* Mol Psychiatry, 2020.
16. Stokes, L., et al., *P2X4 Receptor Function in the Nervous System and Current Breakthroughs in Pharmacology.* Front Pharmacol, 2017. **8**: p. 291.
17. Boué-Grabot, É., et al., *Subunit-specific Coupling between γ-Aminobutyric Acid Type A and P2X2 Receptor Channels.* Journal of Biological Chemistry, 2004. **279**(50): p. 52517-52525.
18. Boué-Grabot, É., et al., *Cross-talk and Co-trafficking between ρ1/GABA Receptors and ATP-gated Channels.* Journal of Biological Chemistry, 2004. **279**(8): p. 6967-6975.
19. Toulmé, E., et al., *An intracellular motif of P2X3 receptors is required for functional cross-talk with GABAA receptors in nociceptive DRG neurons.* Journal of Neurochemistry, 2007. **102**(4): p. 1357-1368.
20. Jo, Y.-H., et al., *Cross-talk between P2X4 and γ-Aminobutyric Acid, Type A Receptors Determines Synaptic Efficacy at a Central Synapse.* The Journal of Biological Chemistry, 2011. **286**(22): p. 19993-20004.
21. Khakh, B.S., et al., *State-dependent cross-inhibition between transmitter-gated cation channels.* Nature, 2000. **406**(6794): p. 405-10.
22. Boué-Grabot, É., et al., *Intracellular Cross Talk and Physical Interaction between Two Classes of Neurotransmitter-Gated Channels.* The Journal of Neuroscience, 2003. **23**(4): p. 1246-1253.

23. Emerit, M.B., et al., *A New Mechanism of Receptor Targeting by Interaction between Two Classes of Ligand-Gated Ion Channels.* The Journal of Neuroscience, 2016. **36**(5): p. 1456-1470.
24. Soto, P., et al., *Function of P2X4 Receptors Is Directly Modulated by a 1:1 Stoichiometric Interaction With 5-HT(3)A Receptors.* Front Cell Neurosci, 2020. **14**: p. 106.
25. Gordon, G.R., et al., *Norepinephrine triggers release of glial ATP to increase postsynaptic efficacy.* Nat Neurosci, 2005. **8**(8): p. 1078-86.
26. Pougnet, J.-T., et al., *ATP P2X Receptors Downregulate AMPA Receptor Trafficking and Postsynaptic Efficacy in Hippocampal Neurons.* Neuron, 2014. **83**(2): p. 417-430.
27. Pougnet, J.-T., et al., *P2X-mediated AMPA receptor internalization and synaptic depression is controlled by two CaMKII phosphorylation sites on GluA1 in hippocampal neurons.* Scientific Reports, 2016. **6**: p. 31836.
28. Pankratov, Y., et al., *P2X receptors and synaptic plasticity.* Neuroscience, 2009. **158**(1): p. 137-48.
29. Khakh, B.S., et al., *Neuronal P2X transmitter-gated cation channels change their ion selectivity in seconds.* Nat Neurosci, 1999. **2**(4): p. 322-330.
30. Krupp, J.J., et al., *Calcium-dependent inactivation of recombinant N-methyl-D-aspartate receptors is NR2 subunit specific.* Molecular Pharmacology, 1996. **50**(6): p. 1680-1688.
31. Zheng, X., et al., *Ca2+ Influx Amplifies Protein Kinase C Potentiation of Recombinant NMDA Receptors.* The Journal of Neuroscience, 1997. **17**(22): p. 8676-8686.
32. Michailidis, I.E., et al., *Phosphatidylinositol-4,5-Bisphosphate Regulates NMDA Receptor Activity through α-Actinin.* The Journal of Neuroscience, 2007. **27**(20): p. 5523-5532.
33. Royle, S.J., L.K. Bobanović, and R.D. Murrell-Lagnado, *Identification of a Non-canonical Tyrosine-based Endocytic Motif in an Ionotropic Receptor.* Journal of Biological Chemistry, 2002. **277**(38): p. 35378-35385.
34. Royle, S.J., et al., *Non-canonical YXXGΦ endocytic motifs: recognition by AP2 and preferential utilization in P2X4 receptors.* Journal of Cell Science, 2005. **118**(14): p. 3073-3080.
35. Pankratov, Y.V., U.V. Lalo, and O.A. Krishtal, *Role for P2X Receptors in Long-Term Potentiation.* The Journal of Neuroscience, 2002. **22**(19): p. 8363-8369.
36. Mizuno, T., I. Kanazawa, and M. Sakurai, *Differential induction of LTP and LTD is not determined solely by instantaneous calcium concentration: an essential involvement of a temporal factor.* Eur J Neurosci, 2001. **14**(4): p. 701-8.
37. Huganir, R.L. and R.A. Nicoll, *AMPARs and synaptic plasticity: the last 25 years.* Neuron, 2013. **80**(3): p. 704-17.
38. Toulmé, E., et al., *Functional Properties of Internalization-Deficient P2X4 Receptors Reveal a Novel Mechanism of Ligand-Gated Channel Facilitation by Ivermectin.* Molecular Pharmacology, 2006. **69**(2): p. 576-587.
39. Richler, E., E. Shigetomi, and B.S. Khakh, *Neuronal P2X2 receptors are mobile ATP sensors that explore the plasma membrane when activated.* J Neurosci, 2011. **31**(46): p. 16716-30.
40. Bobanovic, L.K., S.J. Royle, and R.D. Murrell-Lagnado, *P2X Receptor Trafficking in Neurons Is Subunit Specific.* The Journal of Neuroscience, 2002. **22**(12): p. 4814-4824.
41. Popova, M., et al., *Residues in Transmembrane Segments of the P2X4 Receptor Contribute to Channel Function and Ethanol Sensitivity.* Int J Mol Sci, 2020. **21**(7).
42. Davies, D.L., et al., *Ethanol differentially affects ATP-gated P2X(3) and P2X(4) receptor subtypes expressed in Xenopus oocytes.* Neuropharmacology, 2005. **49**(2): p. 243-53.
43. Ogata, J., et al., *Effects of Anesthetics on Mutant N-Methyl-d-Aspartate Receptors Expressed in Xenopus Oocytes.* Journal of Pharmacology and Experimental Therapeutics, 2006. **318**(1): p. 434-443.